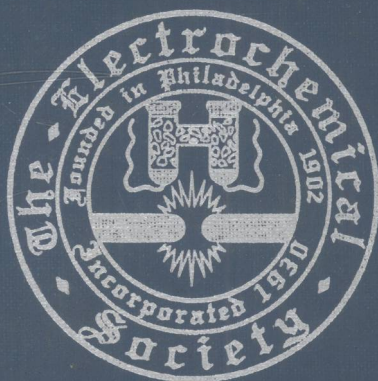


FUNDAMENTAL ASPECTS OF HIGH TEMPERATURE CORROSION



Edited by

D. A. Shores
R. A. Rapp
P. Y. Hou

TG172-53

9870490

F981

1996

PROCEEDINGS OF THE SYMPOSIUM ON

FUNDAMENTAL ASPECTS OF HIGH TEMPERATURE CORROSION

Editors

D.A. Shores

University of Minnesota

Minneapolis, Minnesota

R. A. Rapp

The Ohio State University

Columbus, Ohio

P. Y. Hou

Lawrence Berkeley Laboratory

Berkeley, California



E9860490

HIGH TEMPERATURE MATERIALS AND CORROSION DIVISIONS

Proceedings Volume 96-26



THE ELECTROCHEMICAL SOCIETY, INC.,
10 South Main St., Pennington, NJ 08534-2896

Copyright 1997 by The Electrochemical Society, Inc.
All rights reserved.

This book has been registered with Copyright Clearance Center, Inc.
For further information, please contact the Copyright Clearance Center,
Salem, Massachusetts.

Published by:

The Electrochemical Society, Inc.
10 South Main Street
Pennington, New Jersey 08534-2896, USA

Telephone (609) 737-1902
Fax (609) 737-2743
e-mail: ecs@electrochem.org
Web site: <http://www.electrochem.org>

ISBN 1-56677-126-9

Printed in the United States of America

Preface

This volume contains the papers offered at the symposium on Fundamental Aspects of High Temperature Corrosion at the 190th meeting of the Electrochemical Society in San Antonio, Texas on October 8-9, 1996. It also contains two papers that were scheduled, but could not be presented.

It is sometimes said that "fundamentals" do not change. This symposium has been presented six times over approximately the past fourteen years. From the volume published in 1986 the major topics were: oxidation and sulfidation, mixed oxidant attack, hot corrosion, scale adherence, and experimental techniques. Perhaps not too surprisingly, these same topics could also have been used as sub-headings in the present volume. However, one should not infer from this a lack of progress in the field. The contents of several of the present papers demonstrate evidence of considerable progress in advancing techniques (one example is several new X-ray based techniques involving fluorescence, reflection and diffraction were described). Reflected in the current volume is evidence of an expanding interest in stresses and cracking of oxide scales that involves both theoretical and experimental approaches. New developments in coatings and coating techniques to protect novel metallic and intermetallic alloys are also described. Progress continues.

The editors wish to thank all the authors for preparing excellent contributions and for submitting them in a timely fashion.

David A. Shores

Peggy Y. Hou

December, 18, 1996

FACTS ABOUT THE ELECTROCHEMICAL SOCIETY, INC.

The Electrochemical Society, Inc., is an international, nonprofit, scientific, educational organization founded for the advancement of the theory and practice of electrochemistry, electrothermics, electronics, and allied subjects. The Society was founded in Philadelphia in 1902 and incorporated in 1930. There are currently over 7000 scientists and engineers from more than 60 countries who hold individual membership; the Society is also supported by more than 100 corporations through Patron and Sustaining Memberships.

The Technical activities of the Society are carried on by Divisions and Groups. Local Sections of the Society have been organized in a number of cities and regions.

Major international meetings of the Society are held in the Spring and Fall of each year. At these meetings, the Divisions and Groups hold general sessions and sponsor symposia on specialized subjects.

The Society has an active publications program which includes the following:

Journal of The Electrochemical Society - The **Journal** is a monthly publication containing technical papers covering basic research and technology of interest in the areas of concern to the Society. Papers submitted for publication are subjected to careful evaluation and review by authorities in the field before acceptance, and high standards are maintained for the technical content of the **Journal**.

Interface - Interface is a quarterly publication containing news, reviews, advertisements, and articles on technical matters of interest to Society Members in a lively, casual format. Also featured in each issue are special pages dedicated to serving the interests of the Society and allowing better communication between Divisions, Groups, and Local Sections.

Meeting Abstracts (*formerly Extended Abstracts*) - Meeting Abstracts of the technical papers presented at the Spring and Fall Meetings of the Society are published in serialized softbound volumes.

Proceedings Series - Papers presented in symposia at Society and Topical Meetings are published from time to time as serialized Proceedings Volumes. These provide up-to-date views of specialized topics and frequently offer comprehensive treatment of rapidly developing areas.

Monograph Volumes - The Society has, for a number of years, sponsored the publication of hardbound Monograph Volumes, which provide authoritative accounts of specific topics in electrochemistry, solid state science, and related disciplines.

For more information on these and other Society activities, visit the ECS Home Page at the following address on the World Wide Web:

<http://www.electrochem.org>.

TABLE OF CONTENTS

The Critical Strain Energy Criterion For Oxide Spallation - Revisited H.E. Evans and A. Strawbridge	1
Numerical Analysis of the Effects of Substrate Corners and Interface Convolution on Residual Stresses in Oxide Scales R.L. Williamson and J.K. Wright	16
Interface Convolution and Its Effect on Alumina Scale Spallation P.Y. Hou, R.M. Cannon, H. Zhang, and R.L. Williamson	28
Determination of Stress Gradients in Oxidized Ni-Cr Alloy Substrates by in-situ X-ray Diffraction D. Zhu, J.H. Stout, and D.A. Shores	41
Strain Measurements in Thermally Grown Alumina Scales Using Ruby Fluorescence D. Renusch, B.W. Veal, K. Natesan, I. Koshelev, and M. Grimsditch	62
The Morphology of Al ₂ O ₃ Scales: Indicators of Phase, Growth Mechanisms, and Grain Boundary Segregation B.A. Pint	74
Refracted X-ray Fluorescence (RXF) Applied to the Study of Thermally Grown Oxide Scales I. Koshelev, A.P. Paulikas, and B.W. Veal	86
Grain Boundary Segregation of Cation Dopants in α -Al ₂ O ₃ Scales B.A. Pint and K.B. Alexander	97
Application of Pulsed Laser Deposition of Mullite Diffusion Barriers for SiC-C/C Composites in Oxidizing Atmospheres H. Fritze, J. Jojic, T. Witke, C. Rüscher, S. Weber, S. Scherrer, B. Schultrich, and G. Borchardt	109
Oxidation and Pore Formation at the Mullite/SiC Interface in Air and Water Vapor K.N. Lee, E.J. Opila, and R.A. Miller	124
The Effects of Alumina Coatings on the Oxidation of Ni-20Cr J.M. Hampikian, M.R. Hendrick, and W.B. Carter	139
Enhanced Growth of Surface Oxide Layers During Oxidation of Some Metals in Atomic Oxygen S.A. Raspopov, A.A. Vecher, A.G. Gusakov, A.G. Voropayev, M.L. Zheludkevich	151
Comparing the Oxidation Rates of SiC Before and After Oxide Devitrification L.U.J.T. Ogbuji and D.L. Humphrey	163

Oxidation Behavior of Cr-Cr ₂ Nb Alloys P.F. Tortorelli and B.A. Pint	174
Early Stages in the High Temperature Cyclic Oxidation of β -NiAl: An X-ray Reflectivity Study G. Muralidharan, X.Z. Wu, H. You, A.P. Paulikas and B.W. Veal	186
High Temperature Oxidation of Platinum-Aluminum Alloys M. Nanko and T. Maruyama	198
The Effects of Porous Reactive Oxide Coatings on the Formation of Al ₂ O ₃ Scale on Nb ₂ Al-NbAl ₃ Intermetallic Alloys T. Hayashi, T. Maruyama, and K. Nagata	209
Influence of Yttrium on Chromia Scale Growth on Ni-Cr Alloys D. Zhu, J.H. Stout, and D.A. Shores	220
The Effect of Chlorine on Mixed Oxidant Corrosion W.T. Bakker	241
Formation of Carbon Coatings on Silicon Carbide by Reactions in Halogen Containing Media I.D. Jeon, M.J. McNallen, and Y.G. Gogotsi	256
Volatile Hydroxide Species of Common Protective Oxides and Their Role in High Temperature Corrosion E.J. Opila and N.S. Jacobson	269
Electrical Conductivity of Undoped and Doped NiO at Low Oxygen Pressures (Approximately 10 ⁻⁵ to 10 ⁻⁹ Atm): Evidence of P Type to N Type Transition in NiO Y.W. Shin and J.B. Wagner, Jr.	281
Evaluation of Oxidation Damage in Thermal Barrier Coating Systems D. Zhu and R.A. Miller	289
Effects of Mo-Al Coating on Sulfidation Behavior of 310 Stainless Steel W. Kai, Y.J. Wu, J.P. Chu, and P.Y. Lee	308
Influence of Carbon Dioxide on Corrosion Behavior of Stainless Steel in Molten Lithium-Sodium Carbonate K. Matsumoto and K. Nakagawa	320
The Corrosion of Fe-18Al and Fe-18Al-2Nb in H ₂ /H ₂ S/H ₂ O Mixed-Gas Environments W. Kai, R.T. Huang, J.P. Chu, and P.Y. Lee	332
Oxidation of S-Doped β -NiAl in H ₂ /H ₂ O and in Air K. Prüssner, E. Schumann, and M. Rühle	344

THE CRITICAL STRAIN ENERGY CRITERION FOR OXIDE SPALLATION - REVISITED

H E Evans and A Strawbridge

School of Metallurgy and Materials
The University of Birmingham
Birmingham B15 2TT
UK

The critical strain-energy criterion (CSEC) requires that the strain energy stored in the oxide layer during cooling is released by interfacial crack growth only at the critical temperature drop at which spallation occurs. Finite element methods are used to show that this seemingly unlikely behaviour is approximated when creep relaxation in the alloy substrate inhibits the growth of the interfacial wedge crack. Under these conditions, an extensive period of zero crack growth can result during cooling, particularly for alloys of low creep strength and/or low cooling rates. At lower temperatures, when creep processes are limited, crack growth continues. Such cracking kinetics are shown to apply to both chromia- and alumina-forming alloys.

INTRODUCTION

High-temperature alloys are designed for oxidation protection through the early formation of a dense, surface layer which is usually chromia or alumina. The growth rates of such protective oxides are low and acceptable periods of high temperature exposure can be achieved provided that spallation of the oxide layer does not occur. Such spallation to the oxide/metal interface will expose regions of the underlying alloy which have been depleted of beneficial elements, e.g. chromium or aluminium, and which experience difficulty in re-forming the protective oxide. In such locations, metal wastage rates can be orders of magnitude larger than those under the protective oxide. Clearly, it is important to be able to predict the spallation characteristics of a given oxide/substrate system but, as will be shown in this paper, this cannot be done reliably without knowledge of the deformation and cracking processes involved.

Particular attention will be paid in the paper to the concept of the *critical strain-*

energy criterion (1) (subsequently termed CSEC) that envisages oxide spallation to occur when the strain energy within the oxide layer exceeds the energy required to produce fracture at the oxide/metal interface. This strain energy can derive from both growth and differential thermal strains but spallation is usually observed when the oxide layer experiences in-plane compressive (rather than tensile) stresses (2). For most oxide/metal systems, compressive thermal stresses are produced during cooling from the oxidation temperature. The CSEC has proved to be an influential concept and has been applied (3-9) to many oxide/metal systems in attempts to predict both the initiation of spallation and the quantity of oxide subsequently released.

It will be demonstrated that the underlying arguments behind the CSEC are not intuitively reasonable but the potential usefulness of the approach as a predictive tool merits a re-examination of the concept. Essential to this process will be the use of finite element methods to model interfacial crack growth between oxide and alloy substrate (10). Before proceeding to this, it will first be useful to review current understanding of spallation mechanisms from flat surfaces. To accord with usual experience, spallation will be considered only during cooling when typical protective oxide layers experience in-plane compressive stresses.

SPALLATION OF OXIDE LAYERS UNDER COMPRESSION

To effect spallation at the oxide/metal interface it is necessary to develop cracks through the thickness of the oxide layer and to develop a zone of decohesion at the interface (4). In oxide/metal systems having intrinsically poor scale adhesion, a zone of decohesion may well develop during isothermal oxidation as a result of void formation at the oxide/metal interface (11). Additionally, the segregation of sulphur and other elements to the interfacial region can occur (12,13) and this is also likely to impair adhesion. Over such an area of decohesion oxide buckling is possible in principle, as shown in Figure 1(a). Through-thickness cracking of the oxide is then initiated in regions of high convex curvature and localised spallation results. For many years, this was the traditional model (14,15) for oxide spallation but it is now recognised to be inconsistent with the behaviour of alloys designed for high temperature service. In such alloys, additions of rare-earth elements e.g yttrium, will greatly reduce the extent of interfacial voidage and of sulphur segregation, and long-term exposure conditions will lead to protective oxide layers of many microns in thickness. The combined effect of reducing the radius, c , of the zone of initial decohesion and increasing oxide thickness, ξ , is to increase the temperature drop, ΔT_b , to initiate spallation to unrealistically high values according to:

$$\Delta T_b = \frac{1.22}{\Delta \alpha (1 - \nu_{ox}^2)} \left(\frac{\xi}{c} \right)^2 \quad [1]$$

where $\Delta \alpha$ is the difference between metal and oxide thermal expansion coefficients and ν_{ox} is the Poisson's ratio of the oxide. This equation assumes (4) that the oxide layer deforms elastically and behaves as a clamped plate under negligible stress prior to cooling. Using typical values of $c = 1 \mu\text{m}$ (i.e. $1 \times 10^{-6} \text{m}$), $\xi = 5 \mu\text{m}$, $\nu_{ox} = 0.3$ and $\Delta \alpha = 8 \times 10^{-6} \text{K}^{-1}$ gives excessively high values ($4 \times 10^6 \text{K}$) for ΔT_b . Indeed, to obtain a reasonable value for this critical temperature drop of say 1000K would require an equally unrealistically (for high-temperature alloys) large radius of the zone of decohesion of some $2000 \mu\text{m}$.

An alternative route to oxide decohesion is by wedging (4) as shown in Figure 1(b). This mechanism is appropriate to thick oxides with an intrinsically strong interface with the alloy, i.e. an interface relatively free of voids. Initial oxide failure by this route is then envisaged to occur by through-thickness shear failure of the compressively-stressed oxide. It is expected that such failure is initiated from pre-existing defects within the oxide layer, either embedded or originating from the oxide surface. The critical, in-plane compressive stress, σ_c , to produce shear cracking from the defect can be expressed generally as:

$$\sigma_c = \frac{K_{IIc}}{f(\pi a)^{1/2}} \quad [2]$$

where K_{IIc} is the critical stress intensity factor for Mode-II shear cracking, a is the half-length of an embedded defect or the length of a surface defect and f is a geometric factor which allows for the orientation of the defect and its length relative to the oxide thickness.

The evaluation of the factor f is far from trivial for the application being considered here but, to first order, a value of unity is reasonable. Similarly, there appears to be no published values of K_{IIc} for naturally-grown oxide layers, although taking $(K_{IIc}/f) \sim 1 \times 10^{-6} \text{N.m}^{-3/2}$ is probably consistent with published values (16-20) for the tensile stress intensity factor K_{Ic} of various oxide layers. This level of uncertainty in these parameters is unwelcome but it is emphasised that only order of magnitude estimates are being sought. If, as earlier, the only significant source of compressive stress is taken to be that due to differential thermal strains (i.e. oxide growth stresses are negligible), then Equation [2] can be modified to give the critical temperature drop, ΔT_c , to induce shear failure of the oxide layer as:

$$\Delta T_s = \frac{(1-\nu_{ox})}{\Delta \alpha E_{ox} (\pi a)^{1/2}} \left(\frac{K_{IIc}}{f} \right) \quad [3]$$

The values of critical temperature drop predicted by this equation for both chromia and alumina are shown in Figure 2 for a range of (surface) defect lengths. In each case, K_{IIc}/f was taken as $1 \times 10^6 \text{ N.m}^{-3/2}$ and other material parameters are as given in Table I. It can be seen that, for both oxides, surface defects longer than about $2 \mu\text{m}$ are predicted to propagate by shear for temperature drops of 100 K or less. These values of ΔT_s are similar to those deduced (4) from thermogravimetric experiments on an austenitic steel. Defect lengths of some microns certainly do exist in thin nominally protective oxide layers (e.g. 16,20) and, as a consequence, can penetrate through a large fraction of the oxide thickness. Such observations will be used in the finite element models described later. It needs also to be recognised that the defect length used in Equation [3] may be a composite value (16-18) which represents the effective length of closely-spaced individual defects. This approach of using a composite defect size seems appropriate when the volume fraction of defects within the oxide layer is relatively small (say $< 10\%$) but fails at much larger values (21).

Table I: Material Parameters used in the Computations

Material	E, GPa	ν	$\alpha \times 10^6 \text{ K}^{-1}$	Fracture Stress, MPa	Expression for Creep Rate, $\dot{\epsilon}$, s^{-1} (σ =stress, Pa; T=temperature, K)
Silica	65.7	0.2	0.5	300	creep rigid
Chromia	260.0	0.3	8.5	n.a.	creep rigid
Alumina	387.0	0.3	7.9	1700	creep rigid
20Cr/25Ni steel	156.8	0.3	17.8	n.a.	$\dot{\epsilon} = 2.10 \times 10^{-28} \sigma^{5.0} \exp(-42100/T)$
Ni16Cr6AlY coating alloy	167.0	0.3	15.2	n.a.	$\dot{\epsilon} = 8.96 \times 10^{-15} \sigma^{3.0} \exp(-35840/T)$
Haynes 214	177.0	0.3	20.0	n.a.	$\dot{\epsilon} = 9.08 \times 10^{-31} \sigma^{5.24} \exp(-48450/T) + 1.65 \times 10^{-15} \sigma^{6.24} \exp(-106030/T)$

The formation of the through-thickness shear cracks creates the necessary geometry for the subsequent growth of a wedge crack along the oxide/metal interface. The wedging process is facilitated, during further cooling, by the sliding

of blocks of oxide along the plane of the shear cracks in the sense shown in Figure 1(b). The proximity of the wedge crack to the alloy substrate suggests that creep relaxation in the alloy of crack-tip stresses will occur and this has been confirmed by recent finite-element analyses (10,22). Such creep interactions preclude the use of linear elastic fracture mechanics although, as implied above, their use within the creep-rigid oxide layer is justifiable. The wedge cracking process in this context is not amenable to analytical treatment although it has been suggested (4) that the critical strain-energy criterion (CSEC) may offer an adequate approximation.

THE CRITICAL STRAIN-ENERGY CRITERION (CSEC)

In the original formulation of the CSEC (1), it was assumed that during cooling, the elastic strain energy stored within the oxide layer was totally available at some critical temperature drop, ΔT_c , to produce decohesion at the oxide/metal interface and cause spallation. The concept has proved popular because it offers some physical basis to the spallation problem but, since no cracking mechanism is identified, the approach is entirely phenomenological. Understanding can then be illusory. An important objective of this present paper is to examine an earlier suggestion (4) that wedge cracking is an appropriate mechanism to be described by the CSEC. Buckling failure, as discussed earlier, will not be a candidate since much of the strain energy produced during cooling is contained within the buckle configuration and does not contribute to the cracking process. Mathematical development of the CSEC in the absence of a cracking model can be undertaken readily.

For an oxide layer of thickness ξ , a spacing between shear cracks of λ and a strain energy within unit volume of oxide of W^* , the maximum energy available within the oxide layer bounded by the shear cracks is $\lambda^2 \xi W^*$. The CSEC requires that this energy produces failure at the oxide/metal interface over an area λ^2 , i.e.

$$\lambda^2 \xi W^* = \lambda^2 \gamma_F \quad [4]$$

so that the critical condition becomes:

$$W^* = \frac{\gamma_F}{\xi} \quad [5]$$

where γ_F is the effective interfacial fracture energy. It is important to recognise that this is an effective value since, even in the absence of a crack, a fraction of the

energy stored in the oxide will be dissipated by creep of the alloy substrate (23). In the presence of an interfacial crack this energy dissipation will be more evident as will be discussed in the section on finite-element modelling.

The strain energy within the oxide layer is taken to derive solely from the in-plane differential cooling strains, ϵ_{ox} , given as:

$$\epsilon_{ox} = -\Delta\alpha\Delta T \quad [6]$$

where $\Delta T (=T_{\text{initial}} - T)$ is the temperature drop expressed as a positive number. Assuming that the oxide layer experiences equal biaxial stresses, σ_{ox} , the strain energy per unit volume is given as (4):

$$W^* = \frac{1}{2}\sigma_{ox}\epsilon_{ox} + \frac{1}{2}\sigma_{ox}\epsilon_{ox} = \frac{E_{ox}}{(1-\nu_{ox})} \Delta\alpha^2 \Delta T^2 \quad [7]$$

Substitution of Equation [7] into [5] then gives the critical temperature drop, ΔT_c , for spallation as (4):

$$\Delta T_c = \left(\frac{\gamma_F}{\xi E_{ox} (\Delta\alpha^2) (1-\nu_{ox})} \right)^{1/2} \quad [8]$$

This derivation assumes negligible oxidation growth stresses, i.e. the oxide is free of stress prior to cooling. This will be a good approximation where unconstrained metal section thicknesses are small and/or when the alloy creep strength is low, since creep relaxation will be possible at the oxidation temperature. High creep strength alloys of thick section are likely to develop growth stresses during oxidation and the above derivation would then need to be used with caution.

The striking feature between Equation [8] and that for buckling (Equation [1]) is in the dependence of ΔT on oxide thickness. A consequence is that, unlike buckling, the CSEC predicts that spallation will become easier as oxide thickness increases. This is a commonsense expectation but, of more significance, it has also been shown (24) that Equation [8] describes measured ΔT_c values for a chromia layer on a 20Cr25Ni austenitic steel, as shown in Figure 3. This is currently the most extensive data set available. In this figure, the line drawn through the data represents the best fit of Equation [8] and corresponds to a value of γ_F of 6 J.m⁻². Although there is much data scatter, the trend of decreasing ΔT_c with increasing oxide thickness is evident and contrasts with the rising trend expected of buckling

(Equation [1]). The spall morphology was also as expected from a wedging mechanism (25), i.e. isolated regions of spalled oxide (typically 10-20 μm in diameter) with inclined fracture surfaces with the residual adherent oxide as depicted in Figure 1(b). Similar spall morphologies have been reported for the same alloy oxidised at higher temperature (26) and for an alumina layer on a nickel-based alloy (20).

It is evident that the CSEC is capable of describing spallation but, intuitively, it is not reasonable that it should do so. The difficulty is that the CSEC requires no cracking until the temperature has reached ΔT_c to give the kinetics of interfacial crack growth shown in Figure 4. However, it has already been shown that nucleation of the wedge crack by propagation of through-thickness shear cracks is likely to occur early during cooling (Figure 2) and must be associated with the release of some of the stored strain energy. A crude but adequate estimate of this can be obtained from the fracture mechanics approach used earlier. Thus, within the spirit of this approximation, let the geometric factor f equal unity so that the value of $K_{Ic} = 10^6 \text{ N.m}^{3/2}$. The energy, U , dissipated in producing two new crack faces of length w along the perimeter 4λ is approximated by:

$$U = 4\lambda w \frac{K_{Ic}^2}{E_{ox}} \quad [9]$$

For notional values of $w = 1 \mu\text{m}$ (i.e. the residual thickness of oxide underneath a defect in the oxide layer), $\lambda = 15 \mu\text{m}$ (typical length of a spalled area) and $E_{ox} = 387 \text{ GPa}$ (the value for alumina from Table 1) gives $U = 1.6 \times 10^{-10} \text{ J}$. The total strain energy developed in the same volume of oxide during cooling is given from Equation [7] as:

$$W^* = \lambda^2 \xi \frac{E_{ox}}{(1-\nu_{ox})} \Delta \alpha^2 \Delta T^2 \quad [10]$$

Again using representative values of $\xi = 5 \mu\text{m}$, $\Delta \alpha = 8 \times 10^{-6} \text{ K}^{-1}$ and $\Delta T = 400 \text{ K}$ gives $U = 6.4 \times 10^{-9} \text{ J}$. This comparison serves to show that the shear cracking process is likely to release only a small percentage (in the above example, some 2.5%) of the total strain energy developed within the oxide layer on cooling to the spallation temperature. This loss is a second order effect and, as such, will not affect the general usefulness of the CSEC.

A more significant concern is the requirement, shown in Figure 4, that the

interfacial crack should grow instantaneously at the spallation temperature. Such growth kinetics can be found in the catastrophic failure of brittle materials but ought not to be expected for oxide spallation at high or intermediate temperatures where slow crack growth and creep relaxation processes are likely to occur. This apparent inconsistency between the required cracking kinetics and the ability of the CSEC to describe spallation by wedging can be resolved through finite element modelling of the wedging process.

FINITE ELEMENT MODELLING

Initial finite element modelling of spallation by wedge cracking was reported in 1993 (10) and applied to a chromia layer on an austenitic steel. In a later paper (22), the same mesh geometry was used to extend the analysis to alumina-forming ferritic steels. These and new results on alumina-forming nickel-based alloys will be considered in this section.

The numerical model considers spallation to occur over a circular zone of radius r contained within a spall cell of radius R (Figure 5). Axisymmetric, cylindrical geometry is used throughout. The thickness of the substrate alloy is 190 μm . The finite element mesh in the vicinity of the spall zone is shown in Figure 6. An important feature of the model is the use of interfacial elements (27) of high aspect ratio for the shear crack and the interfacial zone. These can be given different physical and mechanical properties from the oxide and alloy substrate. In particular, they can be allowed to fail at defined values of the tensile stress acting normal to the plane of the element. In some cases, e.g. chromia on a silicon-bearing steel (10), the oxide/metal interface, along which cracking takes place, is amorphous silica and is given appropriate properties (Table 1). In the absence of a distinct phase, the interface can be given the properties of the surface oxide (22). Another feature of the interfacial elements is that they can represent a shear crack by having zero shear modulus but non-zero Young's modulus. Normal forces can then be transmitted across the crack surfaces. In the present model, these interfacial elements are 0.1 μm thick. The 45° shear crack (see Figure 6) is assumed to penetrate to the oxide/metal interfacial zone, i.e. for the 5 μm thick surface oxide layer being considered, the shear crack has a length of 7.07 μm . The oxide/metal interfacial elements are each 1 μm long and so the wedge crack increases in length by 1 μm as each crack-tip element fails. All the oxide layers considered here are taken to be creep rigid during cooling but the alloy substrates are generally allowed to creep according to the algorithms given in Table 1. These show the creep rate to be highly temperature dependent, as shown in Figure 7, so that at some stage during cooling, the substrate will also become creep rigid. In this analysis it is then assumed to deform elastically. The double term used to describe creep in the Haynes 214 alloy represents the decrease in creep strength

that occurs at high temperatures when the γ' strengthening phase is in solution.

Predictions of the critical temperature drop, ΔT_c , to initiate spallation for the 20Cr25Ni steel cooling from 900°C (1173K) at 100 K/h are shown as a function of chromia thickness in Figure 8 (10). Also shown are the 95% confidence limits to the thermobalance data given in Figure 3. Although these computations were performed for an initial temperature of 900°C and the data refer to 850°C (1123K), it is known (28) that similar spallation results are obtained from each temperature. These bounds to the data reflect an inverse square root dependence of ΔT_c on oxide thickness as given by the CSEC (Equation [8]). It can be seen that the predictions assuming elastic behaviour of the steel substrate provide poor agreement with the experimental data both in absolute values and in the parametric dependence of ΔT_c on oxide thickness. The CSEC evidently does not apply in this case. On the other hand, when alloy creep deformation is considered, both the numerical and parametric agreement is satisfactory. More detailed computations of the strain energy released during spallation have been performed (10) and confirm that the CSEC holds to a good approximation in this system if the alloy substrate is permitted to creep. Why should this be so?

The reason can be understood from a comparison of the growth kinetics of the interfacial wedge crack as shown for this 20Cr25Ni steel in Figure 9. Under elastic conditions, the growth of the wedge crack occurs continuously with increasing displacement along the inclined shear crack bounding the spall zone. This displacement derives, of course, from the differential thermal contraction strains during cooling. When the substrate is permitted to creep, however, the wedge crack blunts shortly after its nucleation and a delay in subsequent growth develops as shown in Figure 9. Growth of the crack continues when creep relaxation rates in the alloy become low as cooling continues. As a consequence of creep relaxation, the kinetics of growth of the wedge crack resemble those expected (Figure 4) if the CSEC were to hold. Thus, since the loss of strain energy in developing the shear cracks is small, then to first order, the accumulated oxide strain energy is released in crack propagation over a relatively small temperature drop. It must be remembered, of course, that much can also be lost in creep relaxation prior to crack growth but this fraction is accommodated in the effective fracture energy, γ_F .

This influence of creep is duplicated in the other examples considered in this paper as shown in Figure 10 for the alumina-forming Haynes 214 and the Ni16Cr6AlY coating alloy. For each alloy, the initial oxidation temperature was taken as 1100°C (1373K) and different pairs of cooling rates are considered. Even for the highest rate (10⁶ K/h in Figure 10(b)), a measurable delay in wedge crack growth is still predicted. The cracking kinetics of the Haynes alloy (Figure 10(a)) closely follows that expected from the CSEC, such that the crack growth stage extends over only some 10% of the total temperature drop. This rapid rate of

growth reflects the high creep strength developed at temperatures less than about 840°C (1113K), Figure 7, and also the large difference ($12.1 \times 10^{-6} \text{ K}^{-1}$) in thermal expansion coefficients for this system (Table 1). A final point to note from Figure 10 is that propagation of the shear crack and nucleation of the wedge crack occur at temperature drops in the range 50-100K and, thus, accord with expectations (Figure 2).

Therefore, for all cases which have been studied to date, the influence of substrate creep is to delay the growth of the interfacial wedge crack. The extent of this delay, in terms of ΔT , depends on the intrinsic creep strength of the alloy and also on the cooling rate. The influence of the latter for the Ni16Cr6AlY with a 5 μm alumina surface layer cooling from 1100°C is shown in Figure 11 (29). The solid curve (creeping alloy) shows how ΔT_c decreases from about 750°C (1023K) to about 315°C (588K) with increasing cooling rate. At the highest rate (10^6 K/h), the value is close to that expected for elastic behaviour (broken line in Figure 11) but some creep relaxation still occurs (Figure 10(b)).

CONCLUSIONS

It is shown that the critical strain-energy criterion is valid only when interfacial crack growth occurs quickly at temperatures close to the final spallation temperature. Finite element methods have been used to demonstrate that this condition can be achieved if the growth stage of a wedge crack at the oxide/metal interface is retarded by creep relaxation within the alloy substrate. These cracking kinetics are most readily achieved at low cooling rates and in alloys whose creep strength is strongly dependent on temperature.

REFERENCES

1. U. R. Evans, *An Introduction to Metallic Corrosion*, p. 194, Edward Arnold, London (1948).
2. H. E. Evans, *Mater. High Temp.*, **12**, 219 (1994).
3. J. Armitt, D. R. Holmes, M. I. Manning, D. B. Meadowcroft and E. Metcalfe, *The Spallation of Steam Grown Oxides from Superheater and Reheater Tube Steels*, Report FP-686, Electric Power Research Institute, Palo Alto, CA (1978).
4. H. E. Evans and R. C. Lobb, *Corros. Sci.*, **24**, 209 (1984).
5. P. W. G. Simpson and H. E. Evans, in *Nuclear Fuel Performance*, p. 265, British Nuclear Energy Society, London (1985).
6. H. E. Evans and R. C. Lobb, in *Eurocorr'87*, p. 135, DECHEMA, Frankfurt